

**Intersystem Crossing Driven by Vibronic Spin-Orbit Coupling:  
A Case Study on Psoralen  
(Electronic Supplementary Information)**

Jörg Tatchen<sup>a</sup> and Natalie Gilka<sup>a</sup> and Christel M. Marian<sup>a\*</sup>

<sup>a</sup> *Institute of Theoretical and Computational Chemistry,  
Heinrich Heine University, Universitätsstr. 1, D-40225 Düsseldorf, Germany*

(Dated: April 26, 2007)

---

\*E-mail: Christel.Marian@uni-duesseldorf.de

## I. IMPACT OF USER-DEFINED PARAMETERS ON THE CALCULATED ISC RATE CONSTANTS

For polyatomic systems with many degrees of freedom, the density of vibrational levels increases drastically with increasing vibrational excitation energy. Of course, radiationless transitions take place isoenergetically and therefore the density of final levels  $|f, \mathbf{v}'\rangle$  at the energy of the initial vibronic level  $|i, \mathbf{v}\rangle$  is decisive. At low adiabatic electronic energy differences, the radiationless transition takes place among only a few vibronic levels. In the absence of subsequent decay channels the state population will be periodically transferred back and forth among the levels. For large electronic energy gaps  $E_i^{ad} - E_f^{ad}$ , the final levels may form a quasi-continuum. Under these conditions, the decay of the initial level appears to take place irreversibly on the time scales which are accessible to experiment. This variety of characteristics of radiationless transitions has been analyzed from a fundamental point of view in the literature (e. g. [1–7]) and a detailed system-independent classification of the possible scenarios (e. g. the small molecule limit or the statistical limit) is available. The applicability of a certain case is usually ascertained on the basis of a few parameters such as the level density and this way a corresponding physical model of the transition is obtained.

Here, we will only partially comment on the above-mentioned limiting cases. Instead, we are interested in the applicability of the interval search algorithm we utilize in the main paper to approximate the Fermi Golden Rule expression for the ISC rate constants  $k_{ISC}$ . According to Toniolo and Persico [8, 9], an energy interval of width  $2\eta$  around the energy  $E_{i, \mathbf{v}=0}$  of the initial level  $|i, \mathbf{v} = 0\rangle$  is scanned for final vibronic levels  $|f, \mathbf{v}'\rangle$ . If we denote the coupling matrix elements driving the radiationless transition by  $V_{\mathbf{v}=0, \mathbf{v}'}$ , the rate constant is obtained as

$$k_{ISC}(i \rightsquigarrow f) = \frac{2\pi}{\hbar\eta} \sum_{|E_{f, \mathbf{v}'} - E_{i, \mathbf{v}=0}| < \eta} |V_{\mathbf{v}=0, \mathbf{v}'}|^2 . \quad (1.1)$$

We investigate the conditions that have to be fulfilled to get rate constants from the interval search algorithm of eq. (1.1) which are numerically stable and hence meaningful.

### A. Impact of the interval width $\eta$

TABLE I: Calculated rate constants  $k_{ISC}$  [ $s^{-1}$ ] (right) for ( $S_1 \rightsquigarrow T_2$ ) ISC channels (left). Remaining columns: adiabatic electronic energy difference  $\Delta E^{ad}$  [eV], direct SOME  $|\langle i|H_{SO}|f\rangle|_{q_0}$  [ $cm^{-1}$ ], number  $\#_{derivs}$  of included derivatives w. r. t. *oop* modes in vibronic SO coupling, number  $\#_{acc}$  of included accepting modes, width  $\eta$  [ $cm^{-1}$ ] of search interval, resulting number  $\#_{v'}$  of final state vibrational levels within search interval.

channel	parameters & settings					results	
		direct SO	vibr. SO	acceptors	interval	levels	rate
$i \rightsquigarrow f$	$\Delta E^{ad}$	$ \langle i H_{SO} f\rangle _{q_0}$	$\#_{derivs}$	$\#_{acc}$	$\eta$	$\#_{v'}$	$k_{ISC}$
$S_1 \rightsquigarrow T_{2x}$	0.52	0.0	17 <sup>ab</sup>	24	0.01	6906	$3.7 \cdot 10^5$
$S_1 \rightsquigarrow T_{2x}$	0.52	0.0	17 <sup>ab</sup>	24	0.1	69087	$7.5 \cdot 10^5$
$S_1 \rightsquigarrow T_{2x}$	0.52	0.0	17 <sup>ab</sup>	24	1.0	690840	$6.8 \cdot 10^5$
$S_1 \rightsquigarrow T_{2x}$	0.52	0.0	17 <sup>ab</sup>	24	10.0	6909313	$8.3 \cdot 10^5$
$S_1 \rightsquigarrow T_{2y}$	0.52	0.0	17 <sup>ab</sup>	24	0.01	6906	$1.3 \cdot 10^5$
$S_1 \rightsquigarrow T_{2y}$	0.52	0.0	17 <sup>ab</sup>	24	0.1	69087	$9.8 \cdot 10^4$
$S_1 \rightsquigarrow T_{2y}$	0.52	0.0	17 <sup>ab</sup>	24	1.0	690840	$9.6 \cdot 10^4$
$S_1 \rightsquigarrow T_{2y}$	0.52	0.0	17 <sup>ab</sup>	24	10.0	6909313	$8.1 \cdot 10^4$
$S_1 \rightsquigarrow T_{2z}$	0.52	$1.0 \cdot 10^{-2}$	0	24	0.01	25	$2.0 \cdot 10^1$
$S_1 \rightsquigarrow T_{2z}$	0.52	$1.0 \cdot 10^{-2}$	0	24	0.1	255	$1.9 \cdot 10^1$
$S_1 \rightsquigarrow T_{2z}$	0.52	$1.0 \cdot 10^{-2}$	0	24	1.0	2736	$8.1 \cdot 10^2$
$S_1 \rightsquigarrow T_{2z}$	0.52	$1.0 \cdot 10^{-2}$	0	24	10.0	27638	$1.6 \cdot 10^2$
$S_1 \rightsquigarrow T_{2z}$	0.52	$1.0 \cdot 10^{-2}$	0	24	100.0	277834	$1.2 \cdot 10^2$
$S_1 \rightsquigarrow T_{2z}$	0.52	$1.0 \cdot 10^{-2}$	0	24	500.0	1577679	$1.3 \cdot 10^2$
$S_1 \rightsquigarrow T_{2z}$	0.52	$1.0 \cdot 10^{-2}$	0	24	1000.0	4487749	$1.7 \cdot 10^2$

*a*: The derivatives of the respective SOMES are computed at the  $S_1$  geometry and w. r. t. the  $S_1$  normal modes.

*b*: A maximum excitation level  $v_\kappa = 1$  was imposed on each *oop* mode for the evaluation of the vibronic spin-orbit coupling.

The effect of various choices for the interval width parameter  $\eta$  is illustrated in Tab. I for the ISC channels ( $S_1 \rightsquigarrow T_2$ ). The calculations have been performed along the same lines as in the

main paper except for the employed values of  $\eta$  and the number  $\#_{acc}$  of accepting modes. The latter has been increased to 24. This way, the density of final levels is increased sufficiently, to allow for the choice of  $\eta = 10^{-2} \text{ cm}^{-1}$  for all three channels. [Applying  $\#_{acc} = 16$ , not a single level would have been selected in case of ( $S_1 \rightsquigarrow T_{2z}$ ) where no low-frequency out-of-plane (*oop*) modes are active.] In addition, the range of  $\eta$  is extended towards larger values by two orders of magnitude up to a value of  $10^3 \text{ cm}^{-1}$ . This turned out to be feasible solely for the channel  $S_1 \rightsquigarrow T_{2z}$ : For the Herzberg-Teller type treatment of the vibronic spin-orbit coupling, excitation of the out-of-plane (*oop*) modes is allowed for. Due to the rather high vibrational level density which results from excitations in the low-frequency *oop* modes, increasing  $\eta$  beyond values of  $10^1 \text{ cm}^{-1}$  would become very demanding for ( $S_1 \rightsquigarrow T_{2x}$ ) and ( $S_1 \rightsquigarrow T_{2y}$ ).

For the channels ( $S_1 \rightsquigarrow T_{2x}$ ) and ( $S_1 \rightsquigarrow T_{2y}$ ) already values of  $\eta \geq 10^{-1} \text{ cm}^{-1}$  yield essentially identical results. Comparison of the values of  $\#_{v'}$  between ( $S_1 \rightsquigarrow T_{\{2x,2y\}}$ ) and ( $S_1 \rightsquigarrow T_{2z}$ ) in Tab. I suggests that this behaviour is indeed due to the increased density of levels in the Herzberg-Teller type treatment which was already noted above. Among the three ( $S_1 \rightsquigarrow T_2$ ) ISC channels,  $S_1 \rightsquigarrow T_{2z}$  shows the largest variation in the rate constant values compiled in Tab. I. Employing interval width parameters from  $10^{-2} \text{ cm}^{-1}$  to  $10^{-1} \text{ cm}^{-1}$  yields rate constants  $k_{ISC} \approx 2 \cdot 10^1 \text{ s}^{-1}$ . For  $\eta = 1.0 \text{ cm}^{-1}$  a sudden increase by almost two orders of magnitude to  $k_{ISC} \approx 8 \cdot 10^2 \text{ s}^{-1}$  is observed. Larger widths  $\eta \geq 10 \text{ cm}^{-1}$  result in intermediate rates of  $k_{ISC} \approx 1.2-1.7 \cdot 10^2 \text{ s}^{-1}$ . The pronounced variation of  $k_{ISC}$  for low values of  $\eta$  is due to the rather small number of contributing final levels  $\#_{v'}$  as will be pointed out in detail below.

The top of Fig. 1 shows a portion of the FC spectrum for the  $S_1 \rightsquigarrow T_2$  transition that was obtained assuming a single initial level ( $|S_1, v'\rangle$ , corresponding to  $T = 0 \text{ K}$ ) and accounting for the same 24 active modes that were used in Tab. I. The displayed energy interval ( $\eta = 500 \text{ cm}^{-1}$ ) is centered around the isoenergetic  $S_1 \rightsquigarrow T_2$  transition. The spectrum shows pronounced progression structure. If small values are employed for the interval width  $\eta$ , e. g.  $\eta = 0.1 \text{ cm}^{-1}$ , and the adiabatic energy difference  $E_{S_1}^{ad} - E_{T_2}^{ad}$  is slightly altered, one or a few levels may be accounted for or omitted in an uncontrolled fashion in the interval search. If the coupling of these levels is very strong and contributes a noticeable fraction to the total coupling, the obtained values for the rate constant  $k_{ISC}$  will be changed drastically. In other words: thinking about the coupling final levels in the corresponding ( $S_1 \rightsquigarrow T_2$ ) ISC as a quasicontinuum seems thus not to be well justified here.

On a larger scale, however, the FC spectrum in Fig. 1 corresponds to a slowly varying FC weighted density of states. In order to motivate this statement, we introduce a function which we

term the accumulation  $f_{FC}(E)$  of FC factors w. r. t. the energy:

$$f_{FC}(E) = \sum_{\{\mathbf{v}' \mid E_{\mathbf{v}=\mathbf{0}}-\eta \leq E_{\mathbf{v}'}-E_{\mathbf{0}'} \leq E\}} |\langle \mathbf{v}' | \mathbf{v} = \mathbf{0} \rangle|^2 . \quad (1.2)$$

Throughout, the independent variable  $E$  is assumed to represent the vibrational excitation energy in the final state. If  $f_{FC}(E)$  is plotted in an energy interval  $[E_{\mathbf{v}=\mathbf{0}} - \eta, E_{\mathbf{v}=\mathbf{0}} + \eta]$ , the average slope of the graph in this interval is directly proportional to the rate constants  $k_{ISC}$  obtained within the Condon approximation from the interval search algorithm. The calculated rates will be more or less independent of  $\eta$  if  $f_{FC}(E)$  is approximately linear within a not too small region around the energy  $E_{\mathbf{v}=\mathbf{0}}$  of the initial level. Plots of  $f_{FC}(E)$  on two different scales are shown for the ( $S_1 \rightsquigarrow T_{2z}$ ) ISC in Fig. 1. On an enlarged scale (bottom of Fig. 1), sudden changes or discontinuities of the slope of the function  $f_{FC}(E)$  upon variation of  $E$  become apparent. The fluctuations which result in the calculated rates for small values of  $\eta$  can be assigned to the shape of  $f_{FC}(E)$  on this scale. In particular the exceptionally high value of  $k_{ISC}(S_1 \rightsquigarrow T_{2z}) \approx 8 \cdot 10^2 \text{ s}^{-1}$  which is obtained for  $\eta = 1.0 \text{ cm}^{-1}$  is related to the largest step in  $f_{FC}(E)$  which is found in Fig. 1 (bottom). On the reduced scale in Fig. 1 (middle), the sudden jumps still contribute noticeably to the overall increase of  $f_{FC}(E)$  with increasing  $E$ . Quite noteworthy, however, the fluctuations in the rate constant due to contributions of individual levels are evened out for larger interval widths  $\eta \geq 10 \text{ cm}^{-1}$ .

We conclude that numerically stable results for ISC rate constants are obtained from the interval search algorithm if the search interval is chosen in a way so that the function  $f_{FC}(E)$  is sufficiently smooth on the search interval. At the same time, the interval should be narrow enough to ensure that the obtained rate constants are not affected by the global slope of the function  $f_{FC}(E)$ . This global slope is e. g. already becoming apparent in the middle of Fig. 1. It is closely connected to the well-known energy gap law [3, 10, 11] for radiationless transitions:

$$k_{i \rightsquigarrow f} \sim e^{-\alpha \Delta E} \quad \text{with} \quad \alpha > 0 \quad \text{and} \quad \Delta E \equiv (E_{i, \mathbf{v}=\mathbf{0}} - E_{f, \mathbf{v}'=\mathbf{0}}) > 0 . \quad (1.3)$$

Due to the wide range of level densities encountered in ( $S_1 \rightsquigarrow T_n$ ) or ( $T_1 \rightsquigarrow S_0$ ) ISCs, a unique choice of the interval width parameter  $\eta$  seems to be disadvantageous. Instead, we prefer to test the effect of the parameter  $\eta$  for each individual system and to assess sufficient stability of the calculated rate constants by means of checking the functions  $f_{FC}(E)$ . Achieving numerical stability of the rate constants w. r. t. the choice of  $\eta$  for ISC channels driven by vibronic spin-

orbit coupling is in general less demanding due to the increased level density: in fact it should be sufficient that the rate constants obtained within the Condon approximation are stable. Under certain conditions, however, it may turn out to be impossible to obtain stability. The latter applies to situations when the electronic energy gap is very small or even vanishes. In these cases, any separation of the microscopic and global shapes of  $f_{FC}(E)$  becomes meaningless and a linear approximation to  $f_{FC}(E)$  on an intermediate scale is impossible.

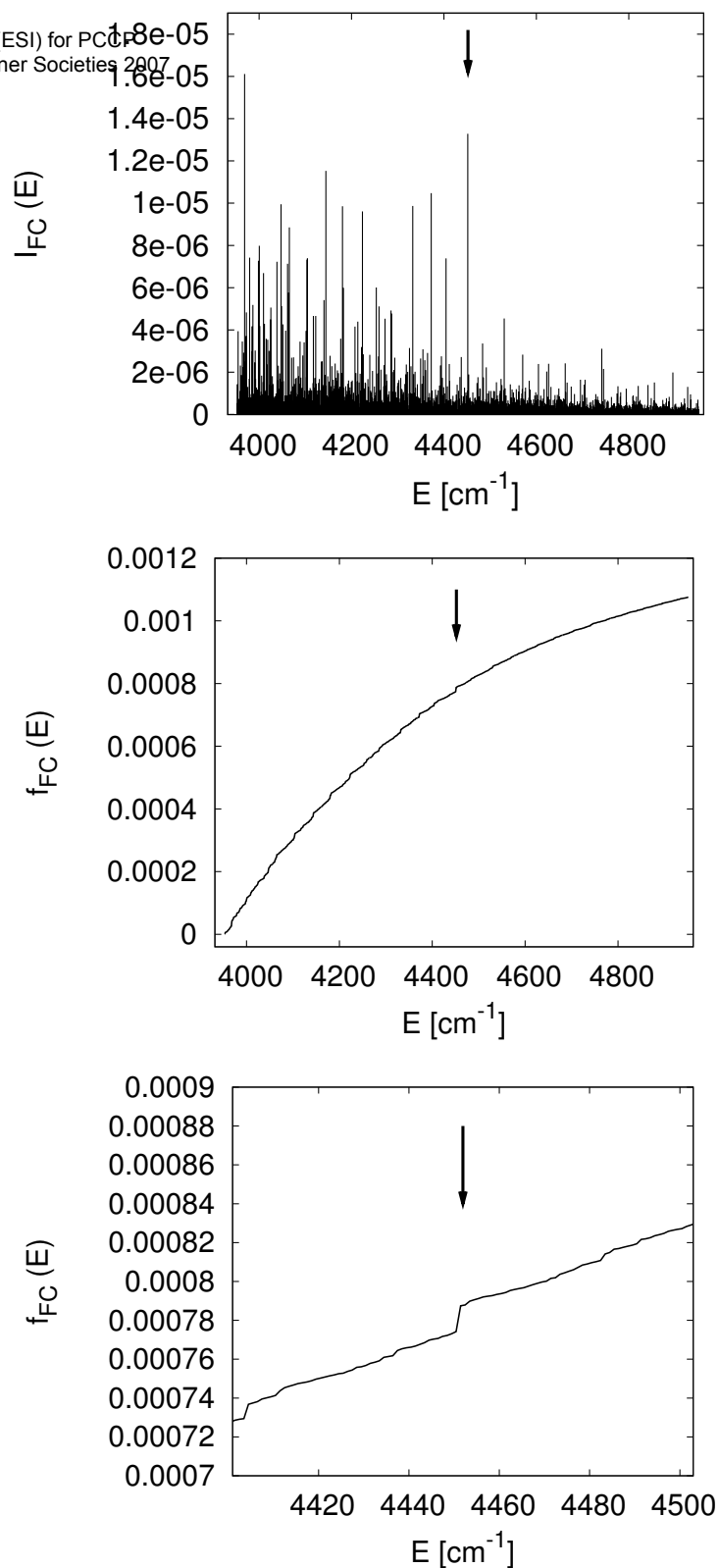


FIG. 1: Visualization of the FC-weighted DOS (truncated to  $\#_{acc} = 24$ ) for ( $S_1 \rightsquigarrow T_{2z}$ ) ISC. Top: ( $S_1 \rightarrow T_2$ ) FC spectrum in an energy interval  $[E_{S_1, \mathbf{v}=0} - \eta; E_{S_1, \mathbf{v}=0} + \eta]$  with  $\eta = 500 \text{ cm}^{-1}$ . Middle: accumulation of FC factors in the same interval. Bottom: same accumulation of FC factors in a smaller interval with  $\eta = 50 \text{ cm}^{-1}$ . The abscissa  $E = E_{T_2, \mathbf{v}' } - E_{T_2, \mathbf{0}' }$  refers to the vibrational excitation energy in the  $T_2$  state. The energetic location of  $|S_1, \mathbf{v} = \mathbf{0}\rangle$  is indicated by a vertical arrow.

## B. Impact of the number of accepting modes $\#_{acc}$

Tab. II shows the dependency of the calculated rate constant  $k_{ISC}$  for the ISC ( $S_1 \rightsquigarrow T_{1z}$ ) on the number  $\#_{acc}$  of totally symmetric accepting modes of the final state which have been accounted for in the calculation. Both the Doktorov method and the displaced oscillators model have been applied. For the latter, the vibrational frequencies and normal modes of the final state ( $T_1$ ) have been employed. The corresponding accumulations of FC factors  $f_{FC}(E)$  for both approaches are shown in Fig. 2. We note that the rate constant in the displaced oscillators model is completely converged with 37 active totally symmetric acceptors because *oop* modes do not contribute here.

The capability of the individual modes to act as an energy acceptor is assessed by means of the dimensionless displacement variables  $|\delta_\kappa|$  entering the Dushinsky transformation between the final and initial state normal mode coordinates (compare main paper). In this way, more and more accepting modes may be accounted for upon increasing  $\#_{acc}$  in the same order in which they are regarded to contribute to the rate constant. In Tab. III, a list of all the 37 totally symmetric vibrations is given for the  $T_1$  state of psoralen which is ordered with respect to the displacement values  $|\delta_\kappa|$ . According to Tab. III, the geometric change between the equilibrium geometries of the  $S_1$  and the  $T_1$  states cannot easily be attributed to a single or a few normal modes. Instead, there are not less than 14 modes showing displacements  $|\delta_\kappa| \geq 0.5$ . Noteworthy, the displacement parameters for the high-frequency (C – H)-stretch modes are almost vanishing. Taking  $|\delta_\kappa|$  as a selection criterion, their contribution to the ISC rate constant is thus expected to be negligible.

The data in Tab. II reveal that almost converged results are obtained from the displaced oscillators model with  $\#_{acc} = 22$ . Correspondingly, the accumulations  $f_{FC}(E)$  of FC factors are very similar for  $\#_{acc} = 22$  and  $\#_{acc} = 37$  in Fig. 2 (bottom). The curves for  $\#_{acc} = 34$  and  $\#_{acc} = 37$  are in fact indistinguishable. Similar statements apply to the results from the Doktorov approach. Nevertheless, the results obtained with  $\#_{acc} = 37$  will not be completely converged here: frequency changes and Dushinsky rotations between *oop* modes in the  $S_1$  and  $T_1$  states may contribute to some extent. We expect this effect to be marginal, however. The choice  $\#_{acc} = 16$  which has been employed in the main paper does in fact not yield fully converged results. From Tab. II and Fig. 2, we estimate that we probably underestimate the rate by approximately a factor of two if we apply  $\#_{acc} = 16$ . For the evaluation of the vibronic spin-orbit coupling, however, the calculations employing  $\#_{acc} = 16$  and  $\eta = 0.1 \text{ cm}^{-1}$  described in the main paper turned out to be already very time-consuming. We therefore refrained from further increasing the density

of coupling vibrational levels that has to be dealt with. Keeping in mind the uncertainties in the excitation energies and further approximations entering our calculations, an error of a factor of two in the final rate constant seems to be quite acceptable.

TABLE II: Calculated rate constants  $k_{ISC}$  [ $s^{-1}$ ] for ( $S_1 \rightsquigarrow T_{1z}$ ) ISC and number  $\#_{v'}$  of contributing final state vibrational levels depending on the number  $\#_{acc}$  of accepting modes accounted for. The search interval  $\eta = 50 \text{ cm}^{-1}$  is congruent with the plotted regions in Fig. 2. Further settings: adiabatic electronic energy difference  $\Delta E^{ad} = 0.88 \text{ eV}$ , direct SOME  $|\langle i | H_{SO} | f \rangle|_{q_0} = 5.3 \cdot 10^{-2} \text{ cm}^{-1}$ .

$\#_{acc}$	Doktorov approach		displaced oscillators	
	$\#_{v'}$	$k_{ISC}$ [ $s^{-1}$ ]	$\#_{v'}$	$k_{ISC}$ [ $s^{-1}$ ]
6	171	$5.8 \cdot 10^3$	150	$1.3 \cdot 10^4$
8	1147	$2.0 \cdot 10^4$	1025	$3.8 \cdot 10^4$
10	11123	$4.7 \cdot 10^4$	9584	$7.6 \cdot 10^4$
12	21379	$8.7 \cdot 10^4$	18185	$1.4 \cdot 10^5$
14	87830	$1.2 \cdot 10^5$	73318	$2.0 \cdot 10^5$
16	596007	$1.6 \cdot 10^5$	486336	$2.6 \cdot 10^5$
18	790890	$2.0 \cdot 10^5$	639099	$3.2 \cdot 10^5$
20	1283444	$2.3 \cdot 10^5$	1024596	$3.7 \cdot 10^5$
22	1754850	$2.6 \cdot 10^5$	1387981	$4.1 \cdot 10^5$
34	10024877	$3.0 \cdot 10^5$	7600588	$4.7 \cdot 10^5$
37	10113190	$3.3 \cdot 10^5$	7662080	$4.7 \cdot 10^5$

TABLE III: Totally symmetric accepting modes for ( $S_1 \rightsquigarrow T_1$ ) ISC: Harmonic vibrational frequencies  $\bar{\nu}_\kappa$  [ $\text{cm}^{-1}$ ] for the  $T_1$  state and dimensionless displacements  $|\delta_\kappa|$ . All values were obtained at the TDDFT/B3LYP level utilizing TZVP basis sets and belong to the structures described in ref. [12].

$\kappa$	$\bar{\nu}_\kappa$	$ \delta_\kappa $									
30	934.01	1.740	35	1179.78	0.689	43	1451.24	0.320	54	3282.62	0.029
9	387.97	1.272	46	1564.57	0.646	38	1281.95	0.319	24	783.67	0.026
48	1597.36	1.108	20	718.63	0.546	44	1480.53	0.298	53	3253.17	0.007
29	922.07	1.058	16	599.42	0.528	28	888.57	0.202	52	3228.85	0.005
21	740.01	1.056	12	495.15	0.487	40	1341.76	0.172	49	3190.18	0.003
33	1141.64	0.974	8	353.02	0.485	39	1329.11	0.136	50	3209.17	0.003
13	543.91	0.911	45	1533.15	0.440	42	1410.91	0.130	51	3219.09	0.002
32	1112.96	0.795	47	1573.02	0.422	36	1198.88	0.111			
5	237.60	0.764	31	1042.49	0.375	41	1374.91	0.088			
34	1148.53	0.740	37	1257.70	0.323	26	835.51	0.084			

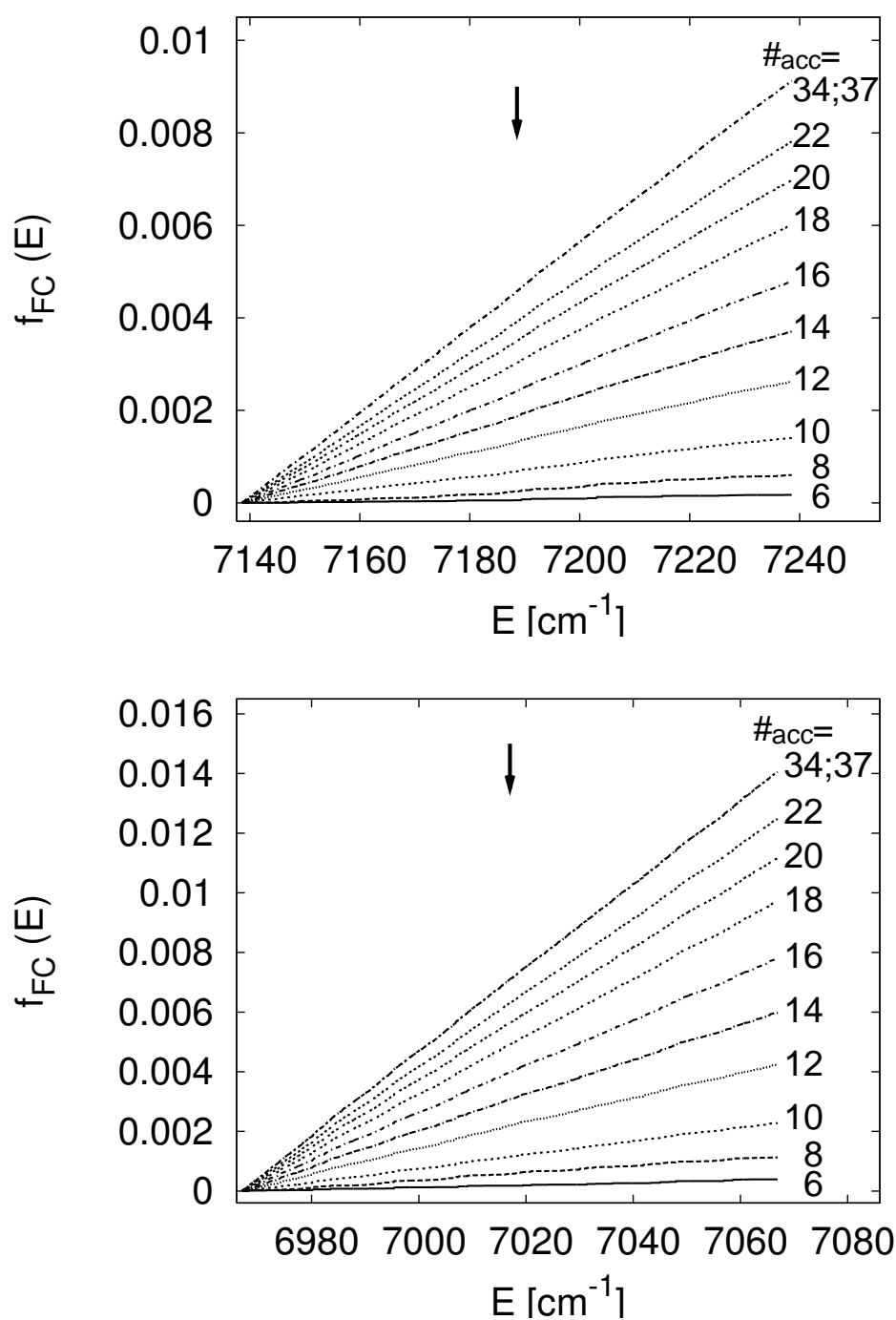


FIG. 2: Impact of the number of active accepting modes  $\#_{acc}$  for ( $S_1 \rightsquigarrow T_{1z}$ ) ISC illustrated by means of accumulations of FC factors. Top: Doktorov FC integrals. Bottom: displaced oscillators model. The abscissa  $E$  refers to the vibrational excitation energy in the  $T_1$  state. The energetic location of  $|S_1, \mathbf{v} = \mathbf{0}\rangle$  is indicated by a vertical arrow. A shift of the displayed energy interval by 172  $\text{cm}^{-1}$  which is noticed comparing the top and bottom graphs is due to the neglect of zero-point vibrational energy changes by the displaced oscillator model.

### C. Maximum excitation degree $v_{oop,\kappa}^{max}$ for the out-of-plane modes

We validate the applicability of rather strict excitation restrictions to the *oop* modes in the evaluation of vibronic spin-orbit coupling by means of a few model calculations. These are accomplished for the ( $S_1 \rightsquigarrow T_{1x}$ ) channel employing a rather low number  $\#_{acc} = 10$  of accepting modes. At the same time, we allow for excitations of only two of the 17 *oop* modes.  $v_{oop,\kappa}^{max} \stackrel{!}{=} 0$  was imposed on all the remaining *oop* modes. [All the derivatives of SOMEs w. r. t. the initial state normal modes enter the calculations. The activity of final state *oop* modes for vibronic spin-orbit coupling is assessed by applying the chain rule to the derivatives of the SOMEs w. r. t. the initial state normal modes. According to this approach, the final state modes 1 ( $\bar{\nu}_1 = 69.1 \text{ cm}^{-1}$ ) and 7 ( $\bar{\nu}_7 = 319.2 \text{ cm}^{-1}$ ) are expected to be the most important ones for vibronic spin-orbit coupling in the case of the channel ( $S_1 \rightsquigarrow T_{1x}$ ).] The maximum excitation degree is then increased from  $v_{oop,\kappa}^{max} = 1$  up to  $v_{oop,\kappa}^{max} = 9$ . According to Tab. IV, essentially converged results are already obtained employing  $v_{oop,\kappa=1,7}^{max} = 1$  for the model chosen. Of course, the rate constant calculated for the model is much lower than the result reported in the main paper. This is due to the different choices which have been applied for  $\#_{acc}$  and the restriction  $v_{oop,\kappa}^{max} \stackrel{!}{=} 0$  that has been imposed on the remaining *oop* modes, here.

TABLE IV: Calculated rate constants  $k_{ISC} [\text{s}^{-1}]$  for ( $S_1 \rightsquigarrow T_{1x}$ ) ISC depending on the maximum excitation degree  $v_{oop,\kappa}^{max}$  for final state *oop* normal modes 1 and 7. Further settings: adiabatic electronic energy difference  $\Delta E^{ad} = 0.88 \text{ eV}$ , derivatives of SOMEs w. r. t.  $S_1$  state normal modes according to Tab. II of the main paper, Doktorov FC integrals, search interval  $\eta = 50 \text{ cm}^{-1}$ .

$v_{oop,\kappa=1,7}^{max}$	$\#_{v'}$	$k_{ISC} [\text{s}^{-1}]$
1	38189	$2.2 \cdot 10^7$
3	113849	$2.4 \cdot 10^7$
5	193844	$2.4 \cdot 10^7$
7	265612	$2.4 \cdot 10^7$
9	326069	$2.4 \cdot 10^7$

- [1] M. Bixon and J. Jortner, *J. Chem. Phys.*, 1969, **50**, 3284.
- [2] M. Bixon and J. Jortner, *J. Chem. Phys.*, 1969, **50**, 4061.
- [3] R. Englman and J. Jortner, *Mol. Phys.*, 1970, **18**, 145–164.
- [4] B. R. Henry and W. Siebrand, John Wiley & Sons, London, 1973; Vol. 1, chapter 4. Radiationless Transitions, pp. 153–237.
- [5] R. Englman, *Non-Radiative Decay of Ions and Molecules in Solids*, North-Holland Publishing, Amsterdam, 1979.
- [6] K. F. Freed in *Radiationless Processes in Molecules and Condensed Phases*, ed. K. F. Freed, Vol. 15 of *Topics in Applied Physics*; Springer-Verlag, Berlin, 1976; chapter 2, pp. 23–168.
- [7] E. S. Medvedev and V. I. Osherow, *Radiationless Transitions in Polyatomic Molecules*, Vol. 57 of *Springer Series in Chemical Physics*, Springer-Verlag, Berlin, 1995.
- [8] A. Toniolo and M. Persico, *J. Chem. Phys.*, 2001, **115**, 1817–1827.
- [9] A. Toniolo and M. Persico, *J. Comput. Chem.*, 2001, **22**, 968–975.
- [10] W. Siebrand, *J. Chem. Phys.*, 1967, **47**, 2411–2422.
- [11] M. Klessinger and J. Michl, *Excited states and photochemistry of organic molecules*, VCH Publishers, Inc., Weinheim, Germany, 1995.
- [12] J. Tatchen and C. M. Marian, *Phys. Chem. Chem. Phys.*, 2006, **8**, 2133–2144.